

## The $\rho$ -inversion and the geyser model for supergiant envelopes

### Abstract:

Firstly, recent improvements in model computations are presented. A major feature, appearing during the evolution of A-M supergiants, is the occurrence of a big density inversion. So to speak, these stars show a thin outer gaseous layer floating upon a radiatively supported zone. The physical causes of the  $\rho$ -inversion are examined and a survey of the literature on the subject is made. A new model is proposed, which we call the geyser model. Due to the very short thermal timescale in the outer layers of supergiants, the ionisation front is able to migrate substantially inwards during the dynamical timescale, so that shell ejections are likely to occur. The shell ejection produces a bluewards shift in the HR diagram with an amplitude and duration depending on the amount of the ejected mass. From model properties and analytical expressions, we estimate the mass of the ejected shell, the rate of mass loss during the ejection, the recovery time between two consecutive ejections as well as the secular average mass loss rates.

### 1. Introduction: recent model developments

Let us briefly present the recent stellar models used to discuss massive star evolution and the properties of supergiants. Very extended grids are now completed over the mass range from 1 to 120  $M_{\odot}$  and for composition  $Z=0.002, 0.005, 0.020$  and  $0.040$ . The tables for massive stars have been published (cf. Maeder, 1990b); the evolution is followed up to the end of C-burning. These models are based on up-to-date physical ingredients. At low  $Z$ , non-solar abundance ratios have been taken, in particular for the ratios O/Fe,  $\alpha$ -nuclei elements/Fe, Na/Fe, Al/Fe etc.... For the 18 main elements, a proper account of the non-solar abundances has been made in the computation of the relevant opacity tables.

The most complete information on mass loss rates by stellar wind is based on observations (IUE,

optical, IR, radio) which are available, though with different accuracies, for stars throughout the HR diagram. Recent compilations and fitting expressions have been given by de Jager et al. (1988). Metallicity effects generally enter the stellar structure mainly through the  $Z$ -dependence of the bound-free and line opacities. In the case of massive stars, such direct structural effects of metallicity are insignificant, since electron scattering is the main opacity source in stellar interiors. Only in the external layers there is a metallicity effect that influences the opacities, and thus the atmospheres and stellar winds. This is the reason why metallicity effects mainly occur in massive stars through stellar winds. Expressions in agreement with the wind models by Kudritzki et al. (1987) are used. For Wolf-Rayet stars, recent works have shown that the mass loss rates depend on their actual masses (cf. Langer, 1989) when hydrogen is no longer present. In the models, these results have been accounted for. For such stars, the effects of their extended atmospheres and optically thick winds have also figured in the calculation of their radius and  $T_{\text{eff}}$ .

In stellar interiors, account is given to the overshooting from convective cores. As mentioned in Maeder & Meynet 1989, an overshooting parameter  $d_{\text{over}}/H_p = 0.25$  is taken. An ensemble of detailed comparisons between theoretical isochrones and cluster sequences in the colour-magnitude diagram of clusters and associations has been performed recently (cf. Maeder, 1990a; Meynet et al. 1990). They confirm remarkably well the validity of the above overshooting parameter for initial masses  $M \geq 1.5 M_{\odot}$ , while models without overshooting are unable to meet the observational requirements.

In the present study, we shall examine what inference for the instabilities and outbursts of supergiants can be drawn from a careful examination and analysis of their outer structure and evolution.

### 2. The density inversion in supergiant envelopes and its physical causes

From the point of view of stellar models, the envelopes of A-M supergiants clearly present a very striking property which differentiates supergiants from other stars and may have a considerable impact on their stability. The models exhibit a strong density inversion appearing around  $\log T_{\text{eff}} = 3.90$  (cf. Fig. 1). For an initial 60  $M_{\odot}$  attaining that stage, the density inversion can reach a factor of 10. For lower masses, it is smaller: for a 15  $M_{\odot}$ , the  $\rho$ -inversion amounts to about 20% only. The  $\rho$ -inversion has been noticed by a number of researchers and a review is made in §3 below.

Firstly, it is to be emphasized, that the  $\rho$ -inversion

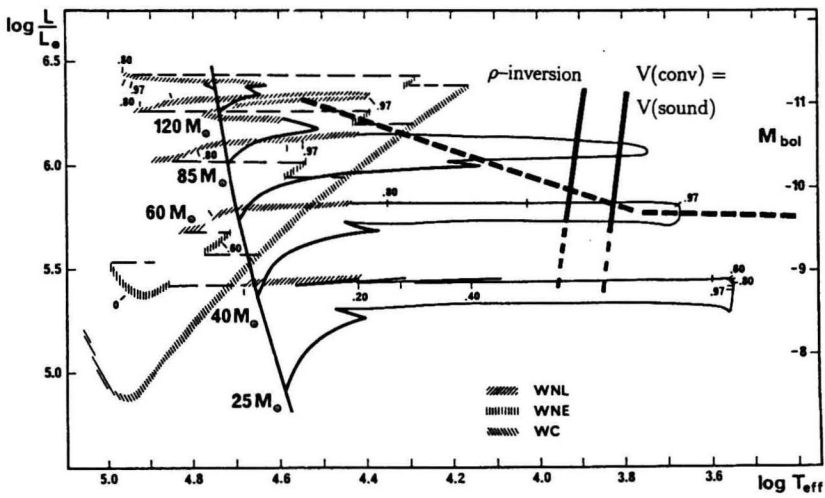


**Figure 1:** Evolutionary tracks in the upper HR diagram for  $Z=0.02$ , with indications (thick lines) of the loci where the density inversion occurs and where convective velocities become sonic. The location of the Humphreys-Davidson limit is shown (broken thick line).

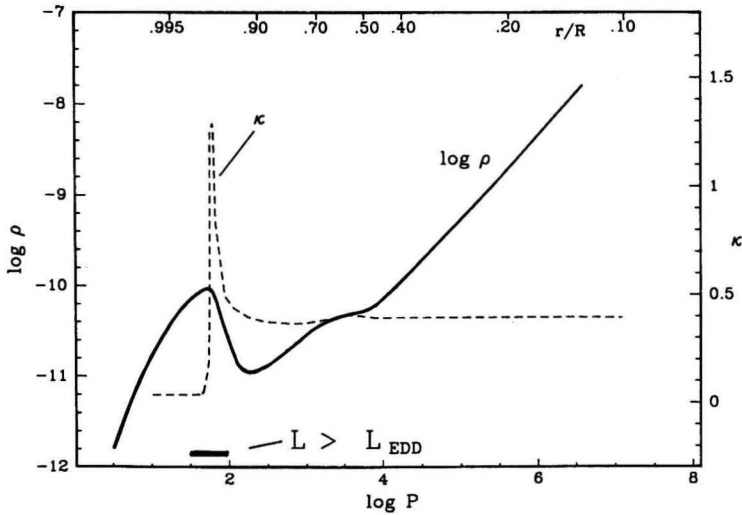


**Figure 2:** The runs of the opacity and density in the outer envelope of a yellow supergiant as a function of pressure and fractional radius. Initial  $60 M_{\odot}$  model as discussed at the beginning of §4.

already appears for subsonic convective velocities, i.e.  $v_{\text{conv}}/v_{\text{sound}} \lesssim 0.1$ . Sonic convective velocities are only reached at a lower  $T_{\text{eff}}$ , i.e. around  $\log T_{\text{eff}} \approx 3.8$  (cf. Fig. 1). Thus, although the  $\rho$ -inversion may be present in regions where the mixing-length theory would predict sonic convective velocities, the primary origin of the density inversion is not due to sonic or nearly sonic convection.

During the evolutionary redwards motion of supergiants, the expansion produces a decrease of temperature and the level at which the ionisation of H occurs goes deeper into the star. At this level, the opacity reaches a strong maximum, which we call opacity-peak (cf. Fig. 2). Near the peak, the actual luminosity is largely above the Eddington-luminosity. In other words, the gradient of radiation pressure ( $-dP_{\text{rad}}/dr$ ) may become large enough, so that

$$\frac{dP_{\text{gas}}}{dr} = -\rho g - \frac{dP_{\text{rad}}}{dr}$$

becomes positive. This occurs when the opacity  $\kappa$  is

$$\kappa > \frac{cg}{\sigma T_{\text{eff}}^4}$$

Thus, the gas pressure increases outwards, i.e.  $dP_{\text{gas}}/dr > 0$ . Due to radiative equilibrium,  $dT/dr$  must be negative and thus one is led to  $d\rho/dr > 0$ , which is a density inversion (cf. Fig. 2). The gas pressure and density are growing outwards. So to speak, the A-M supergiants show an outer gaseous photosphere floating upon a radiative layer.

### 3. Review on the literature about the $\rho$ -inversion and its consequences

The  $\rho$ -inversion has already a long history. So, let us examine some of the various interpretations and consequences, which were proposed.

The precursor finding was published by Underhill (1949) in a study on the early type stars. Although she did not speak about  $\rho$ -inversion, she showed that if the mechanical force exerted by photons exceed gravity, one obtains an outwards growing gas pressure. She suggested that this leads to unstable atmospheres and that the motions would be radial and appearing like prominence action.

Mihalas (1969), referring to the study made by Underhill, showed that the occurrence of an outwards growing gas pressure, joined to the requirement of radiative equilibrium, leads to a strong density inversion. Mihalas suggested that the  $\rho$ -inversion results in a Rayleigh-Taylor instability (RTI), which could be a source of mechanical energy, sufficient to

energize the strong stellar winds of early-type supergiants.

In response to Mihalas' proposal, Kutter (1970) emphasized the need for an hydrodynamic treatment. With the equation

$$\rho \frac{dv}{dt} + \frac{dP_{\text{gas}}}{dr} = -\rho g - \frac{dP_{\text{rad}}}{dr}$$

he found that the positive ( $-dP_{\text{rad}}/dr$ ) leads to a positive outwards acceleration and that there was no density inversion and thus, that no RTI is to be expected. He suggested that the primary mechanism for stellar winds in the early type supergiants is due to the momentum transfer from the radiation field. Coronal mass loss, resulting from a convective zone, was advocated for the late-type supergiants.

In reply to Mihalas' proposal, Wentzel (1970) claimed that the main instability, associated to a  $\rho$ -inversion, is not RTI, but just normal convection. When  $|g_{\text{rad}}|$  exceeds the acceleration of gravity, the density distribution is inverted with respect to the usual gravity vector, but not with regard to the total effective gravity.

Osmer (1972) also found the inversion in gas pressure in a study of F-supergiants. The inversion was found to occur for  $\log g < 1.9$  and mass motions were suggested.

Bisnovatyi-Kogan & Nadyoshin (1972), in a study of yellow supergiants, found the  $\rho$ -inversion and emphasized the impossibility of having convergent static solutions for the atmospheres of these stars. They suggested that matter outflow is the consequence of the excess of luminosity responsible for the  $\rho$ -inversion. They constructed models with hydrostatic cores and hydrodynamically outflowing envelopes at a rate of  $0.5 M_{\odot} \text{yr}^{-1}$ .

Stothers & Chin (1973) did not agree with the previous conclusions and claimed that their more accurate treatment of the static atmospheres always lead to consistent convergent solutions. They suggested that the  $\rho$ -inversion results in turbulent motions that adjust the atmospheric structure appropriately.

There are often numerical difficulties associated to the  $\rho$ -inversion in A to M supergiants, such as trouble to match the outer and inner solutions in hydrostatic models of red supergiants. The use of the density scale height instead of the pressure scale height in the convection theory suppresses the density inversion (cf. Maeder, 1987). The reason is that the convective velocity and flux become large, which herewith reduces the thermal gradient. Such a solution then leads to a slightly bluer location of red supergiants in the HR diagram (cf. Maeder, 1987; Stothers & Chin, 1990). This solution is consistent with the proposals that strong turbulence develops.

However, I would presently consider the above solution as not more than a convenient algorithm to handle supergiant envelopes in a hydrostatic code, but certainly not as a proper solution of the complex hydrodynamics of supergiant envelopes.

The acoustic flux is the dominant mode of energy transport in the outer envelope of red supergiants (cf. Maeder, 1987). For an initial  $60 M_{\odot}$  model, at its reddest point on the evolutionary track in the HR diagram, the acoustic convective and radiative fluxes represent the following fractions of the total flux ( $F_{ac}$ ,  $F_{conv}$ ,  $F_{rad} = (0.91, 0.05, 0.04)$ ) at the point in the star ( $M_r/M = 0.9995$ ) where  $F_{ac}$  is the largest. For a  $15 M_{\odot}$ , at the base of the ascending red giant branch, these values are  $(0.60, 0.27, 0.13)$ . The proper inclusion of the turbulent pressure  $P_{turb}$  and acoustic flux  $F_{ac}$  modifies the envelope structure in a way which limits the growth of the density inversion. This also prevents the convective velocities from being supersonic. The physical cause is that any increase of the convective velocities  $v_{conv}$  makes a much larger  $F_{ac}$  (going like  $v_{conv}^2$ ) which then reduces the thermal gradient and convective velocities.

Recently, Gautschi & Glatzel (1990), in a study of the pulsations of AGB stars, found with an hydrodynamic code that the density inversion is not removed by convection. According to them, the density inversion is unavoidable to maintain the value of the entropy gradient associated to convection. This result is in the line of that of Wentzel.

Thus, from this brief survey of literature, we may identify at least 3 different kinds of conclusions related to the occurrence of a density inversion in the envelopes of supergiants:

- A RTI instability occurs as a result of the  $\rho$ -inversion. The inversion should therefore be washed out by the instability.
- The supra-Eddington-luminosities drive an outwards acceleration and mass. Thus, there is no density inversion appearing.
- Strong convection and turbulence develops and the  $\rho$ -inversion is maintained.

Now, it is clear that the RTI proposal has been disputed with some reason and the other two solutions do not necessarily have the last word. In particular, stellar models (Maeder, 1990) confirm the strong convection and the presence of the  $\rho$ -inversion as in solution 3 above, but simultaneously they also show large supra-Eddington-luminosities, probably able to drive outwards acceleration. Recent hydrodynamical models by Meynet (1990, 1991) well support this view; they show  $\rho$ -inversion, strong convection and simultaneously a rapid outwards accel-

eration of the very outer layers. However, we have still to wait for further modelisations in order to fully describe the dynamical and thermal effects in supergiant envelopes.

#### 4. Timescales and the geyser model

The previous studies generally ignore the various timescales intervening in supergiant envelopes. There are at least 3 different timescales: the dynamical, the thermal and the evolutionary or secular timescales. It is important to carefully discern the values of these timescales in order to thoroughly understand the physics of supergiant envelopes. Below, a simple model is proposed, the geyser model, which is based on a discussion of timescales and structure of the envelopes and suggests cyclic or episodic shell mass ejections, followed by recovery periods which are determined by internal evolution.

Apart from the  $\rho$ -inversion, supergiant envelopes have another essential property. The thermal timescale of the upper layers is very short as shown by Appenzeller (1989) and Maeder (1989). A rough expression for the thermal timescale of a layer of mass fraction  $\Delta M/M$  is

$$t_{\text{therm}} \simeq 3.14 \cdot 10^7 \frac{(M/M_{\odot})^2}{(R/R_{\odot})(L/L_{\odot})} \cdot \frac{\Delta M}{M} \text{ yrs}$$

This expression is obtained assuming that the radiative diffusivity is the same throughout the star. As an example, let us consider a model for an initial  $60 M_{\odot}$  star at an age of  $3.7 \cdot 10^6$  yr, with an actual mass of  $41.4 M_{\odot}$ ,  $\log L/L_{\odot} = 6.05$ ,  $\log T_{\text{eff}} = 3.89$  and  $R = 586 R_{\odot}$ . The time of thermal adjustment for the outer  $10^{-4}$  in mass is 2.9 days and for  $10^{-2}$  it is 292 days. These values mean that the thermal readjustments of the outer layers of supergiants occur very quickly. According to the above expression, for a supergiant of given  $M$  and  $L$ ,  $t_{\text{therm}}$  is shorter for red than for blue supergiants.

Let us recall that the mass fraction above the  $\kappa$ -peak in a yellow supergiant, experiencing the  $\rho$ -inversion, is very small, i.e.  $\Delta M/M = 10^{-6}$  to  $10^{-4}$ . Models by Kutter (1970) or Bisnovatyi-Kogan & Nadyoshin (1972) suggest outwards acceleration and mass outflow as a result of the excess of luminosity responsible for the  $\rho$ -inversion. Recent hydrodynamic models by Meynet (1991) also show fast growing velocities and pulsation in the very outer layers of yellow and red supergiants. Future developments of these models are still needed to follow the detailed hydrodynamics of mass outflows. Now, the important consequence of the very short thermal timescale mentioned above is that, after the possible departure of the very outer layers, any ther-

mal feature, like the ionisation or the Eddington-peak, will be able to move rapidly inwards in lagrangian coordinates (cf. also Fig. 3). Thus, the  $\kappa$ -peak and the associated luminosity excess will be able to accelerate new mass shells as they are rapidly moving deeper into the star.

Some extreme supergiants, like the LBV, are known to experience outbursts and shell ejection (cf. Lamers, 1989; Wolf, 1989; Davidson, 1989). The reason why the mass loss are discontinuous is likely to be related to the values of the various timescales in the supergiant envelope (cf. Maeder, 1989). The basic idea is that during an ejection (the timescale which is of the order of  $t_{\text{dyn}}$ ), the ionisation front and the associated Eddington-peak will move inwards by an amount  $\Delta M$  as large as permitted by the local thermal timescale.  $\Delta M$  is such that

$$t_{\text{therm}}(\Delta M) = t_{\text{dyn}}(\Delta M)$$

i.e. 
$$\Delta M = \frac{RL}{GM} t_{\text{dyn}}(\Delta M)$$

The dynamical timescale  $t_{\text{dyn}}$  corresponding to a shell mass  $\Delta M$  of thickness  $\Delta R$  is

$$t_{\text{dyn}} = (2 \frac{\Delta R}{g})^{1/2} \simeq (2 \frac{R^3}{GM} \frac{\Delta R}{R})^{1/2}$$

Although the peak is close to the surface, the region above the density inversion encompasses nearly 50% of the total stellar radius. We see that  $\Delta R/R \simeq 1/2$  and that this ratio will not greatly change for an increase in  $\Delta M$ . Also, the effective gravity is somehow larger than the surface gravity. Thus, the dynamical timescale will be of the order of

$$t_{\text{dyn}} = \chi (\frac{R^3}{GM})^{1/2}$$

with  $\chi$  between, say, 0.1 and 1 whatever the exact  $\Delta M$  will be. The maximum mass fraction which can therefore be involved in an ejection with a duration  $t_{\text{dyn}}$  is of the order of

$$\frac{\Delta M}{M} = 1.61 \cdot 10^{-12} \chi \frac{R^{3/2} L}{M^{1/2}}$$

where  $R, L$  and  $M$  are in solar units.

For the above numerical example, given for an initial  $60 M_{\odot}$  in the stage of a yellow supergiant with fastly growing  $\rho$ -inversion, one obtains  $\Delta M/M = 0.006$  to  $0.06$  for  $\chi = 0.1$  to  $1$  (compare with Lamers, 1989). Thus, a substantial amount can be ejected within a dynamical timescale, as the Eddington-peak can move on deep enough during that time.

During the ejection event the maximum mass loss rate is just that given by the rate at which the ionisation front is able to progress inwards. This maximum limiting rate is

$$\dot{M} = \frac{\Delta M}{t_{\text{therm}}} = \frac{GM}{RL}$$

In the numerical example showed above, this rate is about  $0.75 M_{\odot} \text{yr}^{-1}$  (compare with Lamers, 1989). We clearly emphasize that this rate applies to the outburst of shell ejection only and is not at all the average secular mass loss rate, which will be estimated below.

Terrestrial geysers, like at Yellowstone, have often a striking properties. After the so-called initial "splash", they continue to eject boiling water and steam for several minutes. The reason is that, after the initial splash, the pressure decreases in the pipe. Very hot water, which was not boiling due to the high pressure in the pipe, starts then boiling and thus ejects the water above. Thus, there is a boiling front moving inwards and sustaining the ejection for some time. In the supergiant model, the equivalent to the boiling front is the ionisation front which quickly moves inwards and brings deeper layers to supra-Eddington-luminosities and outwards acceleration. Below, we shall show another similarity between supergiants and geysers.

#### Average secular mass loss rates and recovery times

With respect to the mass loss rate during a shell ejection, the average secular mass loss rates should of course be smaller by some orders of magnitude. As shown previously by numerical models (cf. Maeder, 1989), the star experiences, after a shell ejection, a rapid shrinkage of the stellar radius (at the dynamical timescale). The star undergoes a bluewards shift in the HR diagram. The amplitude of the shift depends on the amount of mass loss during the ejection, and also whether dust is sufficient to obscure the star or not (cf. Davidson, 1987). As an example, for an initial  $60 M_{\odot}$  star in the yellow supergiant stage, with an actual mass of  $46 M_{\odot}$ , the ejection of a shell with  $1 M_{\odot}$  leads to a shift from  $\log T_{\text{eff}} = 3.82$  to  $\log T_{\text{eff}} = 4.10$  (see Fig. 1).

As shown by numerical simulations of shell ejections, the supergiant after the blue shift moves again slowly to the red, due to its internal secular evolution, which makes the stellar radius increase until a new shell episode occurs again. We may call recovery time  $t_{\text{recov}}$  the time after an ejection for the star to recover the  $T_{\text{eff}}$  which it had just prior to the ejection. Thus, a simple estimate of the average mass loss rate over one such full cycle is



$$\langle \dot{M} \rangle = \frac{\Delta M}{t_{\text{recov}}}$$

Estimates of the recovery time were made for various amounts  $\Delta M$  of mass ejected. For the above numerical example of yellow supergiant, one has

$$\begin{array}{ll} \Delta M = 0.3 M_{\odot} & t_{\text{recov}} = 125 \text{ yr} \\ 1 M_{\odot} & 350 \text{ yr} \\ 3 M_{\odot} & 746 \text{ yr} \end{array}$$

Thus, the average mass loss rate is of the order of  $(1-4) \cdot 10^{-3} M_{\odot} \text{ yr}^{-1}$  with the supposition that the steady rate of mass loss is much smaller (cf. Lamers, 1989).

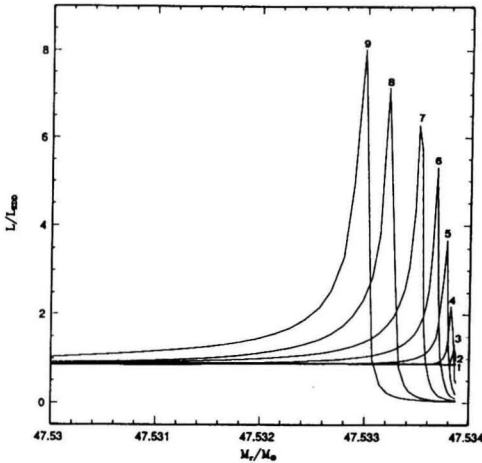


**Figure 3:** Illustration of the inwards migration of the Eddington-peak during the secular evolution of an initial  $60 M_{\odot}$  in the yellow supergiant stage, (see text).

Fig. 3 illustrates the inwards migration of the Eddington-peak in a model of a yellow supergiant evolving in about 280 years from  $\log T_{\text{eff}} = 3.998$  to  $\log T_{\text{eff}} = 3.771$ . We well notice the impressive growth of the Eddington-peak and its inwards motion during the secular evolution.

A few properties of the light variations associated to shell ejection have been identified (cf. Maeder, 1989):

1. The total  $L$  remains nearly constant and the B and V magnitudes change due to the alternation of the bolometric correction during the bluewards and redwards excursions.
2. The amplitudes of the change in  $T_{\text{eff}}$ , and therefore in B and V magnitudes, increase with the  $\Delta M$  ejected.

3. The  $\dot{M}$ -rate during the outburst determines the rate of the initial magnitude variation up to the blue end of the excursion in the HR diagram.
4. The recovery time after an ejection depends on the amount  $\Delta M$  of mass ejected. The average rate of mass loss  $\langle \dot{M} \rangle = \Delta M / t_{\text{recov}}$  does not vary very much with the amount of mass ejected.
5. The shape of the light curve in B or V magnitude also depends on the  $T_{\text{eff}}$  at the time of ejection (due to the bolometric correction).

Interestingly enough, the above models for extreme supergiants share, in addition to the inwards motion of their respective blasting fronts, still another property with terrestrial geysers. As mentioned under point 4 above, longer time intervals between two consecutive ejections are also a common feature to both, the above supergiant model and to the terrestrial geysers.

The results listed above are based on our numerical models of supergiant envelopes and analytical considerations. It is obvious that a complete numerical study of the ejection phases is very needed. Such work is presently undertaken in Geneva thanks to the inclusion by Meynet (1990) of the dynamical acceleration term consistently both in the equations of momentum and energy conservation. These developments are necessary to consider a number of problems in the pre-supernovae stages as well as for the study of several types of instabilities.

#### Acknowledgement:

I thank very much Dr. Georges Meynet for numerous and constructive discussions and information.

#### References

- Appenzeller, I., 1989 "Physics of Luminous Blue Variables" in IAU Coll. 113, Ed. K. Davidson et al., Kluwer Acad. Press, p. 195
- Bisnovatyi-Kogan, G. S., Nadyoshin, D. K., 1972, in *Astrophys. Space Sci.*, **15**, 353
- Davidson, K., 1987, in *Astrophys. J.* **317**, 760
- Davidson, K., 1989 "Physics of Luminous Blue Variables", IAU Coll. 113, Ed. K. Davidson et al., Kluwer Acad. Press, p. 101
- Gautschi, A., Glatzel, W., 1990, *Mon. Not. Roy. Astr. Soc.* **245**, 597
- de Jager, C., Nieuwenhuijzen, H., van der Hucht, K. A., 1988, *Astron. Astrophys. Supp. Ser.* **72**, 259
- Kudritzki, R. P., Pauldrach, A., Puls, J., 1987, *Astron. Astrophys.* **173**, 293

- Kutter, G. S., 1970, *Astrophys. J.* **160**, 369
- Lamers, H., 1989, in "Physics of Luminous Blue Variables", IAU Coll. 113, Ed. K. Davidson et al., Kluwer Acad. Press, p. 195
- Langer, N., 1989, *Astron. Astrophys.* **220**, 135
- Maeder, A., 1987, *Astron. Astrophys.* **173**, 247
- Maeder, A., 1989, in "Physics of Luminous Blue Variables", IAU Coll. 113, Ed. K. Davidson et al., Kluwer Acad. Press, p. 195
- Maeder, A., 1990a, in "Astrophysical ages and dating methods", Ed. E. Vangioni-Flam et al., Ed. Frontières, p. 71
- Maeder, A., 1990b, *Astron. Astrophys. Supp. Ser.* **84**, 139
- Maeder, A., Meynet, G., 1989, *Astron. Astrophys.* **210**, 155
- Meynet, G., 1990, thesis Geneva University
- Meynet, G., 1990, this meeting
- Meynet, G., Mermilliod, J. C., Maeder, A., 1990, in "Astrophysical ages and dating methods", Ed. E. Vangioni-Flam et al., Ed. Frontières, p. 91
- Mihalas, D., 1969, *Astrophys. J.* **156**, L155
- Osmer, P. S., 1972, *Astrophys. J. Supp.* **24**, 255
- Stothers, R., Chin, C. W., 1973, *Astrophys. J.* **179**, 555
- Stothers, R., Chin, C. W., 1990, *Astrophys. J. Supp.* **73**, 821
- Underhill, A. B., 1949, *Mon. Not. Roy. Astr.Soc.* **109**, 562
- Wentzel, D. G., 1970, *Astrophys. J.* **160**, 373
- Wolf, B., 1989, in "Physics of Luminous Blue Variables", IAU Coll. 113, Ed. K. Davidson et al., Kluwer Acad. Press, p. 91

#### *Author's address*

Geneva Observatory, CH-1290 Sauverny, Switzerland